Cardiovascular Research (2011) **92**, 430–438
doi:10.1093/cvr/cvr246

Poly(ADP-ribose) polymerase-2 depletion reduces doxorubicin-induced damage through SIRT1 induction

Magdolna Szántó[1†], Ibolya Rutkai[2†], Csaba Hegedűs[1,3], Ágnes Czikora[2], Máté Rózsahegyi[1], Borbála Kiss[4], László Virág[1,3], Pál Gergely[1,3], Attila Tóth[2], and Péter Bai[1,3*]

[1]Department of Medical Chemistry, Medical and Health Science Center, University of Debrecen, Nagyerdei krt 98. Pf. 7, H-4032 Debrecen, Hungary; [2]Division of Clinical Physiology, Institute of Cardiology, Medical and Health Science Center, University of Debrecen, Debrecen, Hungary; [3]Cell Biology and Signaling Research Group of the Hungarian Academy of Sciences, Debrecen, Hungary; and [4]Department of Dermatology, Medical and Health Science Center, University of Debrecen, Debrecen, Hungary

Received 2 June 2011; revised 27 August 2011; accepted 12 September 2011; online publish-ahead-of-print 15 September 2011

Time for primary review: 33 days

Aims Doxorubicin (DOX) is widely used in cytostatic treatments, although it may cause cardiovascular dysfunction as a side effect. DOX treatment leads to enhanced free radical production that in turn causes DNA strand breakage culminating in poly(ADP-ribose) polymerase (PARP) activation and mitochondrial and cellular dysfunction. DNA nicks can activate numerous enzymes, such as PARP-2. Depletion of PARP-2 has been shown to result in a protective phenotype against free radical-mediated diseases, suggesting similar properties in the case of DOX-induced vascular damage.

Methods and results *PARP-2*$^{+/+}$ and *PARP-2*$^{-/-}$ mice and aortic smooth muscle (MOVAS) cells were treated with DOX (25 mg/kg or 3 μM, respectively). Aortas were harvested 2-day post-treatment while MOVAS cells were treated with DOX for 7 hours. Aortas from *PARP-2*$^{-/-}$ mice displayed partial protection against DOX toxicity, and the protection depended on the conservation of smooth muscle but not on the conservation of endothelial function. DOX treatment evoked free radical production, DNA breakage and PARP activation. Importantly, depletion of PARP-2 did not quench any of these phenomena, suggesting an alternative mechanism. Depletion of PARP-2 prevented DOX-induced mitochondrial dysfunction through SIRT1 activation. Genetic deletion of PARP-2 resulted in the induction of the SIRT1 promoter and consequently increased SIRT1 expression both in aortas and in MOVAS cells. SIRT1 activation enhanced mitochondrial biogenesis, which provided protection against DOX-induced mitochondrial damage.

Conclusion Our data identify PARP-2 as a mediator of DOX toxicity by regulating vascular SIRT1 activity and mitochondrial biogenesis. Moreover, to the best of our knowledge, this is the first report of SIRT1 as a protective factor in the vasculature upon oxidative stress.

Keywords PARP-2 • Doxorubicin • SIRT1 • Mitochondria • Vascular smooth muscle

1. Introduction

Doxorubicin (adriamycin, DOX) is a widely used antitumor drug, exerting cardiovascular side effects that may culminate in irreversible degenerative cardiomyopathy and heart failure.[1] DOX-induced cardiovascular injury is linked to increased oxidative stress[2] as DOX can export electrons from the mitochondria via redox cycling, creating radical species.[3] Although cardiac effects of DOX toxicity are well characterized, vascular damage is scarcely mapped and the molecular background is largely unknown. Vascular damage upon DOX treatment affects the aorta[4,5] and smaller arteries in the liver[6] and kidney.[7,8] Furthermore, DOX impairs endothelial function[9] and promotes thrombosis.[10]

Free radical-evoked DNA damage activates poly(ADP-ribose) polymerase (PARP)-1, which catabolizes NAD^+ in order to create poly(ADP-ribose) (PAR) polymers. PARP-1 activation leads to

[†] These authors contributed equally to this work.

* Corresponding author. Tel: +36 52 412 345; fax: +36 52 412 566, Email: baip@med.unideb.hu

NAD^+ and consequently ATP depletion, provoking cell dysfunction and cell death.[11] This PARP-1-mediated cell death pathway is active in DOX-induced toxicity and it is a major contributor to cardiac and vascular dysfunction.[12,13] Therefore, pharmacological inhibition of PARP-1 proved to be advantageous under such circumstances.[12,13] Upon DOX damage, PARP inhibition partially restored vascular contractility.[13]

PARP-2 is a nuclear enzyme that can bind to DNA nicks and thereby becomes active.[14] Upon activation, it is capable of synthesizing PAR at the expense of NAD^+.[14] Moreover, *PARP-2*$^{-/-}$ mice are resistant to numerous oxidative stress-related pathologies in the brain and intestines.[15–17] These properties of PARP-2 prompted us to examine whether PARP-2 inactivation may also provide protection against DOX-induced vascular damage.

2. Methods

All chemicals were obtained from Sigma-Aldrich unless stated otherwise.

2.1 Animal experiments

All animal experiments were carried out according to the national and EU ethical guidelines and were authorized by the Institutional Ethics Committee (7/2010 DE MÁB). Homozygous female *PARP-2*$^{-/-}$ and littermate *PARP-2*$^{+/+}$ mice[18] derived from heterozygous crossings were kept in a 12/12 h dark–light cycle with *ad libitum* access to water and food. Mice were randomly assigned to four groups: *PARP-2*$^{+/+}$ and *PARP-2*$^{-/-}$ control (CTL), and *PARP-2*$^{+/+}$ and *PARP-2*$^{-/-}$ DOX-treated. DOX treatment was performed by the injection of 25 mg/kg DOX or saline ip as described.[12] Aortas were harvested 2-day post-injection for further assessment.

2.2 Aorta ring studies

For aorta ring studies, mice were anaesthetized by thiopental (50 mg/kg, iv). Mice were dissected after they did not respond to pain. Thoracic aortas were cut into 4 mm rings in an organ chamber and were fixed on an isometric contractile force measurement system (DMT 510A, Aarhus, Denmark) by metal wires. Aortic rings were stretched according to the manufacturer's instructions. Fixed, stretched aortic rings were treated with the indicated agents for the indicated times and contractile force was recorded.

2.3 Histology and microscopy

Staining was performed on 7 μm tissue sections or cells using antibodies against PAR, PARP-2 (both from Alexis, Lausen, Switzerland), and smooth muscle actin (SMA; Novocastra, Newcastle upon Tyne, UK) as in Bai *et al.*[19]

Terminal deoxynucleotidyl transferase dUTP nick-end labelling (TUNEL) assay was performed following the instructions of the manufacturer (Millipore).

2.4 Cell culture

MOVAS murine aortic smooth muscle cells were obtained from ATCC and were cultured in DMEM (4.5 g/L glucose, 10% FCS, and 0.2 mg/mL G418). PARP-2 silencing was performed as in Bai *et al.*[19] employing shPARP-2 (small hairpin) and scPARP-2 (scrambled) shRNA by lentiviral delivery. Cellular measurements took place 7 h after addition of DOX.

2.5 Measurement of thiobarbituric acid reactive species

The extent of oxidative stress was assessed by determining lipid peroxidation. Aortas were homogenized in 1.15% KCl. Homogenates were cleared and supernatants were used. Supernatants were incubated at 90°C for 45 min with thiobarbituric acid. After cooling to room temperature, absorbance at 532 nm was measured and normalized to protein content. The level of lipid peroxides was expressed as a percentage of control.

2.6 PARP activity measurement

PARP activity in MOVAS cells was measured by the incorporation of ^{3}H-NAD^+. Cells stimulated with DOX (3 μM, 7 h) or H_2O_2 (1 mM, 10 min) and were incubated with ^{3}H-NAD^+ (10 min, 37°C). After incubation, cellular proteins were precipitated and subsequently washed with ice-cold TCA (50 and 5% w/v, respectively). Precipitates were solubilized in 250 μL 2% w/v SDS/0.1 N NaOH at 37°C overnight. Tritium incorporation was measured by liquid scintillation counting.

2.7 Measurement of superoxide production

Superoxide was measured using hydroethidine (HE) staining as described in Bai *et al.*[20] Cells were induced by DOX (7 h, 3 μM) and were stained by 2 μM HE for 30 min. Fluorescence was analysed by flow cytometry (FACSCalibur, BD Biosciences). Superoxide production was indicated as a mean of HE fluorescence in each sample.

2.8 Oxygen consumption

Oxygen consumption was measured using an XF96 oximeter (Seahorse Biosciences, North Billerica, MA, USA). scPARP-2 and shPARP-2 MOVAS cells were seeded in 96-well assay plates. After recording the baseline oxygen consumption, cells received a single bolus dose of DOX (0.3–30 μM final concentration). Then, oxygen consumption was recorded every 30 min to follow DOX toxicity. Final reading took place at 7 h post-treatment. The oxygen consumption rate was normalized to protein content and normalized readings were displayed.

2.9 NAD^+ measurement

Cells were seeded in six-well plates and treated with 3 μM DOX for 7 h. Control and DOX-treated cells were homogenized in 500 μL 0.5 N $HClO_4$ solution and the homogenates were then neutralized with 150 μL 3 M KOH. The concentration of NAD^+ was measured photometrically at 560 nm after enzymatic reaction, which is based on an alcohol dehydrogenase cycling reaction in which a tetrazolium dye is reduced by NADH in the presence of phenazine methosulfate. Samples were normalized to protein content and NAD^+ concentration was determined using an NAD^+ standard curve.

2.10 Luciferase activity measurement

Luciferase activity measurement took place as described in Bai *et al.*[19] with modifications as follows. MOVAS cells carrying a stable transfection of a scrambled or specific PARP-2 shRNA were seeded in six-well plates. Transfection took place (8 μg SIRT1 −91 promoter construct[21] and 4 μg β-galactosidase expression plasmid per 9 μL JetPEI transfection reagent (Polyplus Transfection, Illkirch, France) after cells reached ~60% confluence. Cells were scraped 48 h post-transfection and luciferase activity was determined by standard procedures. The activity was expressed as luciferase activity/β-galactosidase activity.

2.11 Measurement of mitochondrial membrane potential

Mitochondrial membrane potential was determined by tetramethylrhodamine ethyl ester (TMRE) staining.[22] MOVAS cells carrying a stable transfection of a scrambled or specific PARP-2 shRNA were seeded in 96-well plate (25 000 cells/well) and induced by DOX (0.3–30 μM, 7 h). After DOX treatment, cells were stained with 25 nM TMRE for 30 min and then were washed with Hanks' balanced salt solution (0.138 M NaCl, 5.33 mM KCl, 0.338 mM Na_2HPO_4, 0.441 mM KH_2PO_4, 1.26 mM $CaCl_2$, 0.493 mM $MgCl_2$, 0.407 mM $MgSO_4$, and

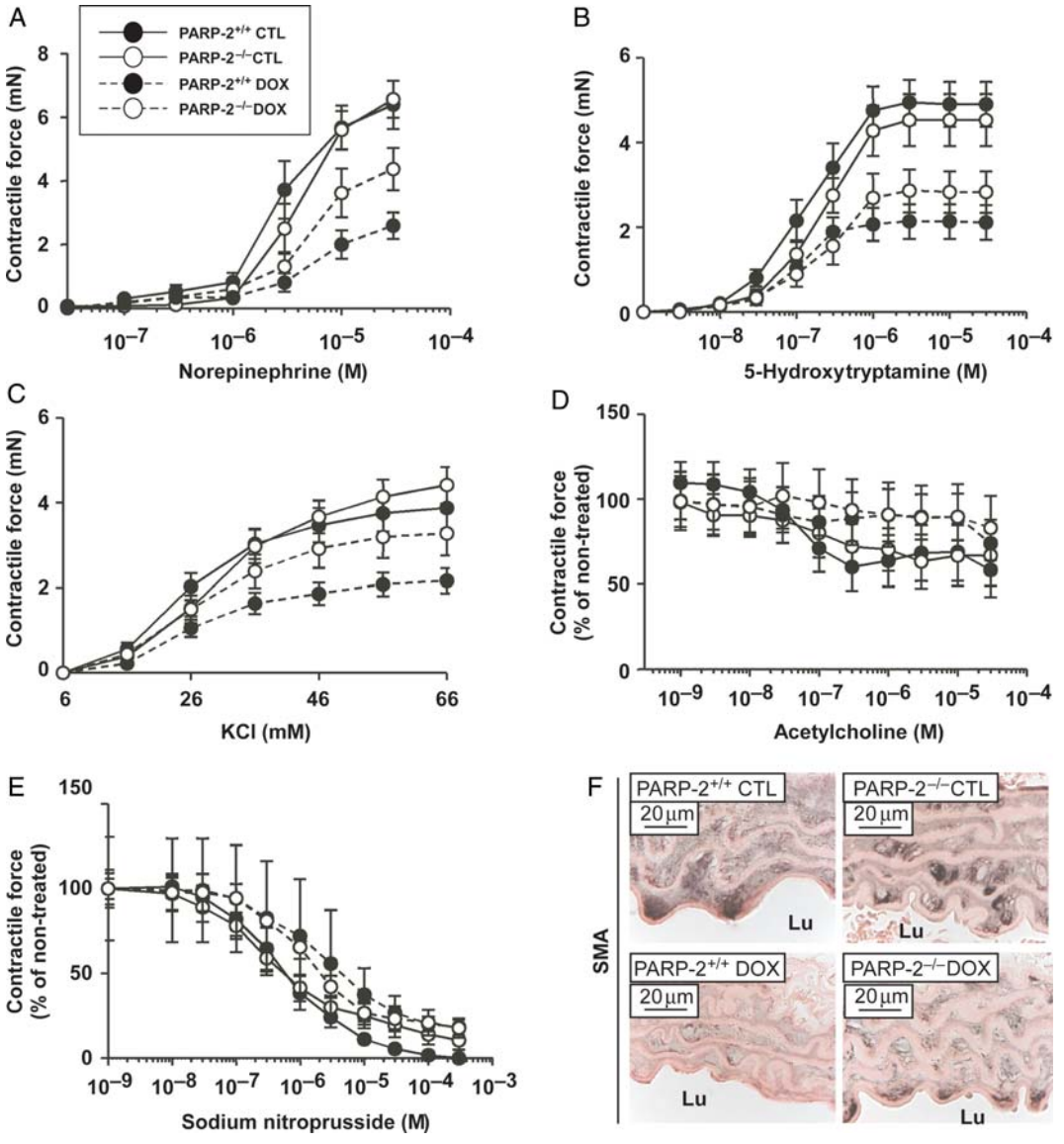

Figure 1 Genetic deletion of PARP-2 protects against DOX-induced aortic dysfunction. *PARP-2*$^{+/+}$ and *PARP-2*$^{-/-}$ mice (3 months of age) were injected with saline (CTL) or with 25 mg/kg DOX ($n = 10$ for *PARP-2*$^{+/+}$ CTL, $n = 7$ for *PARP-2*$^{-/-}$ CTL, $n = 8$ for *PARP-2*$^{+/+}$ DOX, and $n = 8$ for *PARP-2*$^{-/-}$ DOX). Aortas were harvested 2-day post-injection. Aortic rings were mounted on an isometric contractile force measurement system (*A*–*E*) or embedded in paraffin (*F*). Aortic contractile responses (smooth muscle function) were tested by the cumulative application of norepinephrine (*A*), 5-hydroxytryptamine (*B*), and potassium chloride (*C*) and endothelial function was tested by acetylcholine (*D*) and smooth muscle NO sensitivity by sodium nitroprusside (*E*). SMA was visualized by immunohistochemistry (*F*). Luminal side is indicated (Lu), scale bar equals 20 μm.

4.17 mM $NaHCO_3$). Fluorescence was measured on 530 nm as excitation and 590 nm as emission wavelength. TMRE fluorescence was normalized to protein content.

2.12 Protein extraction and western blotting

Cells were lysed with RIPA buffer (1% Nonidet P-40, 1% sodium deoxycholate, 0.1% SDS, 0.15 M NaCl, 0.01 M sodium phosphate, 2 mM EDTA, 50 mM sodium fluoride, and freshly added protease inhibitor cocktail (1:100, Sigma, St Louis, USA). Cells were left on ice for several minutes in the buffer and then were homogenized with a 22 G needle. Lysates were cleared by centrifugation. Extracts were separated by SDS–PAGE and were blotted as in Erdelyi *et al.*[23] Blots were probed with the following antibodies: SIRT1 (1:1000, Millipore-Upstate, Billerica, MA, USA), actin (1:1000, Sigma), and PARP-2 (1:1000, PARP-2, Alexis).

2.13 Total RNA preparation, reverse transcription, and RT-qPCR

Total RNA preparation, reverse transcription, and RT-qPCR were performed similarly as in Brunyanszki *et al.*[24] Total RNA was prepared using TRIzol reagent (Invitrogen) according to the manufacturer's instructions. Two micrograms of RNA were used for reverse transcription (High Capacity cDNA Reverse Transcription Kit, Applied Biosystems, Foster City, CA, USA). Diluted cDNA was used for RT-qPCR. Expression was normalized to the geometric mean of murine 36B4, 18S, and cyclophylin.

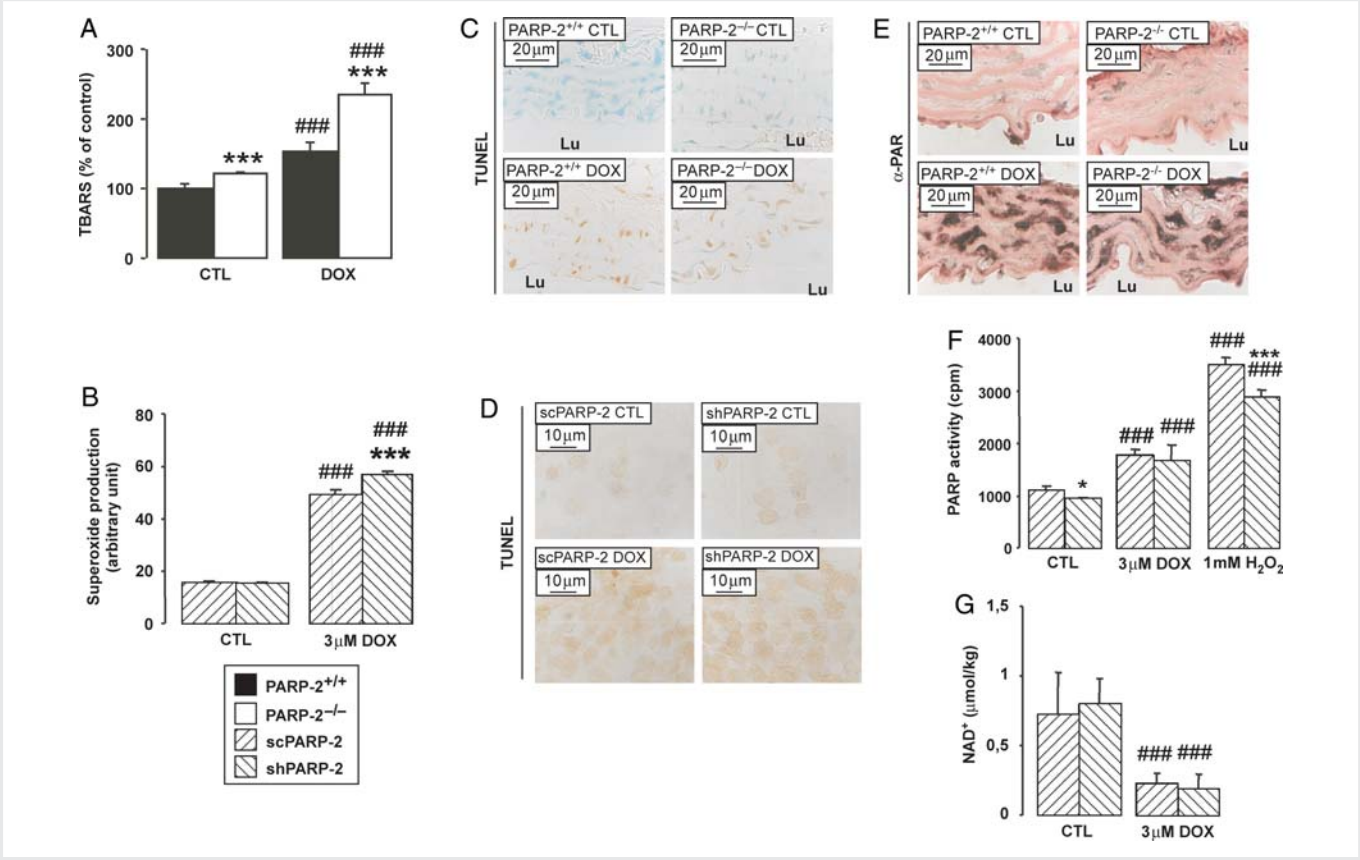

Figure 2 Deletion of PARP-2 does not affect free radical-induced PARP activation or NAD^+ depletion. *PARP-2*$^{+/+}$ and *PARP-2*$^{-/-}$ mice were injected with saline (CTL) or with 25 mg/kg DOX at 3 months of age ($n = 5$ for *PARP-2*$^{+/+}$ CTL, $n = 5$ for *PARP-2*$^{-/-}$ CTL, $n = 5$ for *PARP-2*$^{+/+}$ DOX, and $n = 4$ for *PARP-2*$^{-/-}$ DOX; *A*, *C*, and *E*). An aortic smooth muscle cell line (MOVAS) was also tested (*B*, *D*, *F*, and *G*; $n = 3$ parallel measurements). MOVAS cells were transduced with a PARP-2-silencing (shPARP-2) or -scrambled (scPARP-2) shRNA and treated with solvent (CTL), 3 μM DOX or with 1 mM H_2O_2. Measurements were performed 2-day post-DOX injection (aortas) or 7 h (MOVAS) after DOX treatment. Free radical formation was measured by determining thiobarbituric acid reactive species (TBARS) (*A*) and HE fluorescence (*B*). DNA breaks were detected using TUNEL assay; scale bar represents 20 or 10 μm, respectively (*C* and *D*). PAR formation in paraffin-embedded aortas was assessed with an anti-PAR antibody; scale bar represents 20 μm (*E*), or in MOVAS cells by the PARP enzyme activity assay (*F*). NAD^+ concentrations were determined in MOVAS cells using an alcohol dehydrogenase-coupled colorimetric assay (*G*). Lu, lumen; ### indicate statistically significant difference between CTL and DOX/H_2O_2-treated samples, at $P < 0.001$, * or *** indicate statistically significant difference between *PARP-2*$^{+/+}$ mice/scPARP-2 cells and *PARP-2*$^{-/-}$ mice/shPARP-2 cells at $P < 0.05$ or <0.001, respectively. On (*B*), (*F*), and (*G*), error is represented as SD.

Mitochondrial DNA content was determined in qPCRs using total DNA extract of cells or tissues as described in Bai *et al.*[19] Primers are summarized in Supplementary material online, *Tables S1* and *S2*.

2.14 Chromatin immunoprecipitation

Chromatin immunoprecipitation was performed similarly as in Bai *et al.*[25] In MOVAS cells, chromatin-bound proteins were fixed on DNA by formaldehyde. Nuclei were prepared and chromatin was sonicated in order to split DNA into shorter, ~500 bp fragments. PARP-2-bound chromatin fragments were collected by immunoprecipitation using α-PARP-2 (Alexis) and α-matrix-metalloproteinase-9 (Santa Cruz, Santa Cruz, CA, USA) antibodies. Formaldehyde crosslinking was reversed by heating and then DNA fragments were purified and amplified using SIRT1 promoter-specific primers by qPCR (primers are indicated in the respective section of Supplementary material online). The results were expressed as a percentage of input.

2.15 Statistical analysis

Statistical significance was determined using Student's *t*-test. Error bars represent SEM unless stated otherwise.

3. Results

3.1 PARP-2 depletion counteracts vascular dysfunction

We investigated vascular functions after DOX treatment in *PARP-2*$^{+/+}$ and *PARP-2*$^{-/-}$ mice first. We did not detect major differences in aortic reactivity between untreated (CTL) *PARP-2*$^{+/+}$ and *PARP-2*$^{-/-}$ mice. In contrast, DOX treatment significantly decreased norepinephrine and 5-hydroxytryptamine (serotonin)-induced contractility of the vessels in *PARP-2*$^{+/+}$ mice, while *PARP-2*$^{-/-}$ mice were partially protected (*Figure 1A* and *B*). KCl-induced contraction of aortas from *PARP-2*$^{+/+}$ mice was reduced upon DOX treatment,

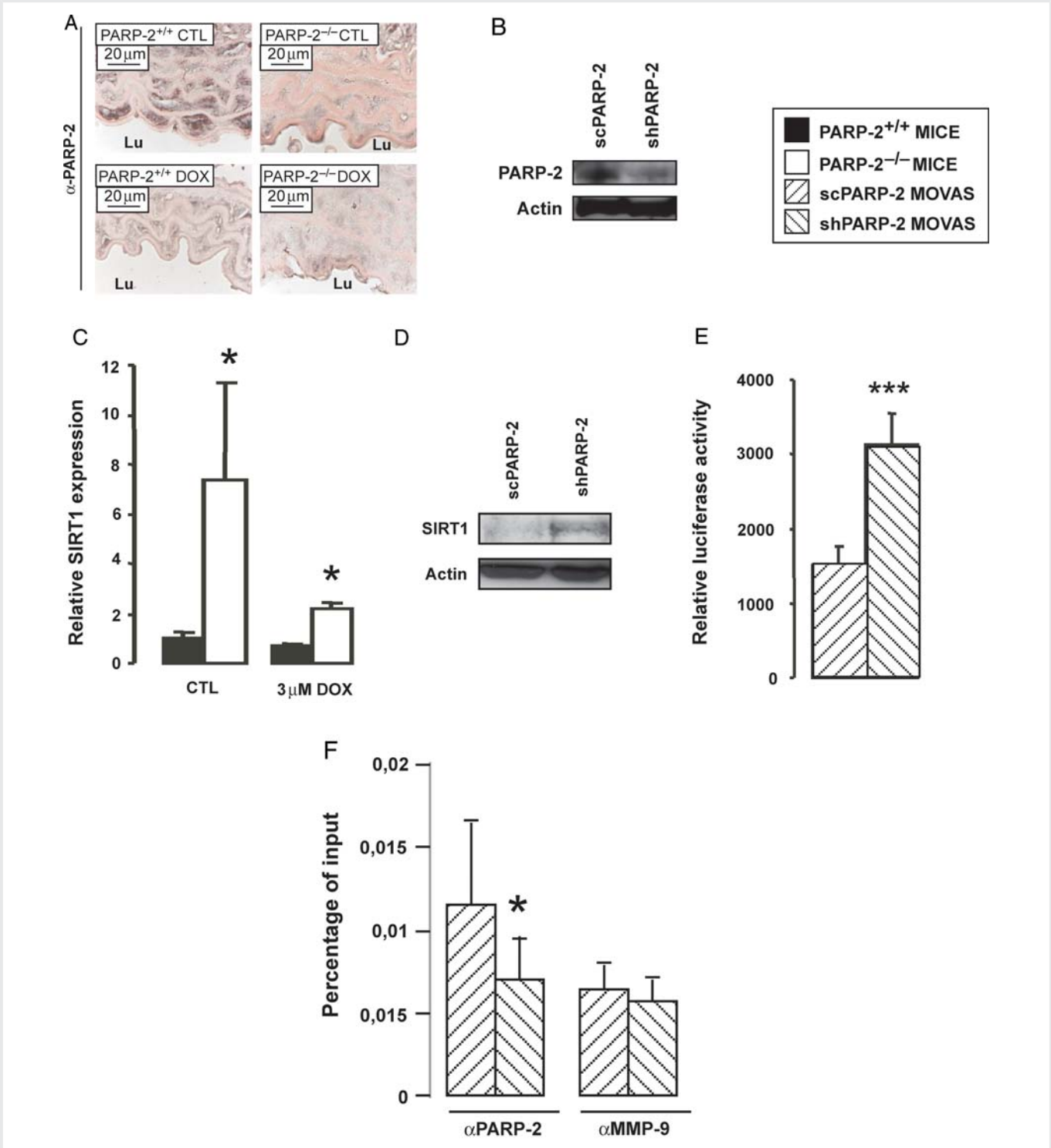

Figure 3 Depletion of PARP-2 induces SIRT1 levels in aortic smooth muscle cells. *PARP-2*$^{+/+}$ and *PARP-2*$^{-/-}$ mice were injected with saline (CTL) or with DOX at 3 months of age ($n = 7$, 5, 5, and 5, respectively), and then aortic samples were collected on day 2 (*A* and *C*). An aortic smooth muscle cell line (MOVAS) was also tested (*B*, *D*, *E*, and *F*). MOVAS cells were transduced with a PARP-2-silencing (shPARP-2) or -scrambled (scPARP-2) shRNA and treated with solvent (CTL) or DOX. PARP-2 expression was determined in aortas by immunohistochemistry, scale bar represents 20 μm (*A*), and in MOVAS cells by western blotting (*B*). SIRT1 expression was determined in aortas by RT-qPCR (*C*), while in MOVAS cells by western blotting (*D*). The activity of the −1 to −91 portion of the SIRT1 promoter was determined in luciferase assays (*E*, $n = 6$). PARP-2 binding to the SIRT1 promoter was determined using ChIP assays (*F*, $n = 3$). Lu, lumen, * and *** indicate statistically significant difference between scPARP-2 cells/*PARP-2*$^{+/+}$ mice and shPARP-2 cells/*PARP-2*$^{-/-}$ mice at $P < 0.05$ or <0.001, respectively. On (*E*) and (*F*), error is represented as SD.

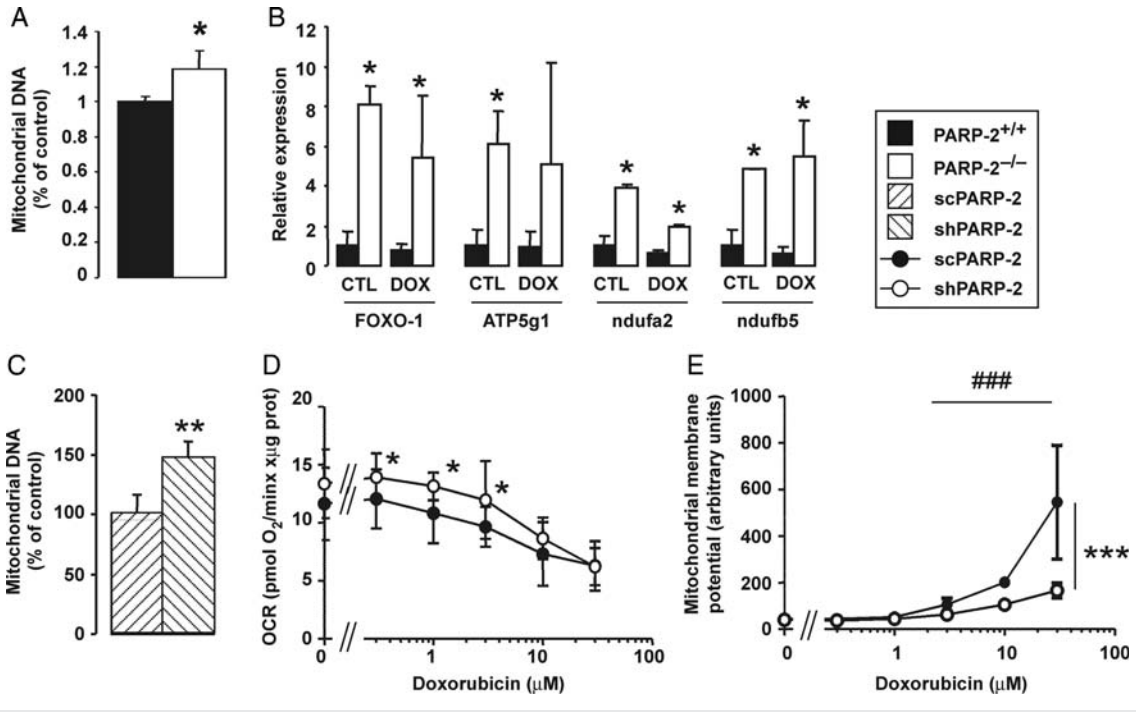

Figure 4 PARP-2 regulates mitochondrial function: possible involvement of SIRT1. *PARP-2*$^{+/+}$ and *PARP-2*$^{-/-}$ mice (3 months of age) were injected with saline (CTL) or with DOX ($n = 7$ for *PARP-2*$^{+/+}$ CTL, $n = 5$ for *PARP-2*$^{-/-}$ CTL, $n = 5$ for *PARP-2*$^{+/+}$ DOX, and $n = 7$ for *PARP-2*$^{-/-}$ DOX), and then aortic samples were collected on day 2 (*A* and *B*). An aortic smooth muscle cell line (MOVAS) was also tested (*C*, *D*, and *E*). MOVAS cells ($n = 3$ parallel measurements) transduced with a PARP-2-silencing (shPARP-2) or -scrambled (scPARP-2) shRNA were treated with solvent (CTL) or DOX. (*A* and *C*) Mitochondrial DNA content was determined by qPCR. (*B*) Expression of a set of mitochondrial genes was determined by RT-qPCR. (*D*) Oxygen consumption rate was measured as described in Section 2 [open symbols represent CTL ($n = 8$); filled symbols represent DOX ($n = 8$)]. (*E*) Membrane potential was determined using TMRE dye. ### indicate statistically significant difference between DOX-treated samples and their respective controls, at $P < 0.001$; *, ** and *** indicate statistically significant difference between *PARP-2*$^{+/+}$ mice/scPARP-2 cells and *PARP-2*$^{-/-}$ mice/shPARP-2 cells at $P < 0.05$, < 0.01 and < 0.001, respectively. On (*C*) and (*D*), error is presented as SD.

whereas the contractile responses of aortas from *PARP-2*$^{-/-}$ mice were unaffected (*Figure 1C*). These findings suggested a PARP-2-dependent deterioration of vascular smooth muscle function after DOX treatment in mice.

Endothelial function was assessed by the application of acetylcholine. Impaired reactivity of aortas to acetylcholine after DOX treatment in both *PARP-2*$^{+/+}$ and *PARP-2*$^{-/-}$ mice indicated that the DOX-induced deterioration of endothelial function was independent of PARP-2 (*Figure 1D*). Moreover, sodium nitroprusside-induced vasorelaxation was not affected by either DOX treatment or by the deletion of PARP-2 (*Figure 1E*), suggesting that blunted acetylcholine responses were not related to impaired NO reactivity of smooth muscle cells.

Taken together, our physiological data suggested a role for PARP-2 in DOX-evoked vascular dysfunction and implicated smooth muscle as a potential target. This notion was further supported by decreased smooth muscle actin (SMA) immunoreactivity in *PARP-2*$^{+/+}$ mice after DOX treatment, suggesting a loss of smooth muscle cells, which was not the case in *PARP-2*$^{-/-}$ mice (*Figure 1F*). Importantly, these data identify smooth muscle dysfunction as a novel mechanism of DOX-induced vascular damage. In our following experiments, we employed an aortic smooth muscle cell line (MOVAS) to reveal the potential mechanisms for PARP-2 involvement in DOX-evoked functional deterioration.

3.2 PARP activity is not altered upon PARP-2 depletion

Reactive oxygen species produced by mitochondrial redox cycling of DOX has previously been shown to trigger PARP activation and PAR synthesis. Moreover, ablation of PARP-1 resulted in suppressed PAR synthesis and protection against DOX-evoked cardiovascular damage.[12,13] Since PARP-2 also possesses PARP activity,[14] we set out to investigate the role of PARP-2 in DOX-evoked PAR synthesis and vascular smooth muscle dysfunction.

We detected free radical production in both aortas and MOVAS cells upon DOX treatment (*Figure 2A* and *B*). Moreover, free radical production was increased upon PARP-2 ablation. Enhanced free radical production resulted in DNA-strand breakage in both types of samples as shown by increased TUNEL staining (*Figure 2C* and *D*). However, there was no apparent change in TUNEL positivity upon PARP-2 ablation or depletion neither in mice nor in MOVAS cells (*Figure 2C* and *D*). The level of DOX-induced PARP activity was not different between *PARP-2*$^{+/+}$ and *PARP-2*$^{-/-}$ mice (*Figure 2E*). Similarly, there was no marked difference in PARP activation between MOVAS cells in which PARP-2 was silenced by specific shRNA (shPARP-2) or its unspecific scrambled version (scPARP-2) (*Figure 2F*). These results suggested a dominant role for PARP-1 in DOX-evoked PAR formation. PAR was detected only in smooth muscle cells, suggesting that

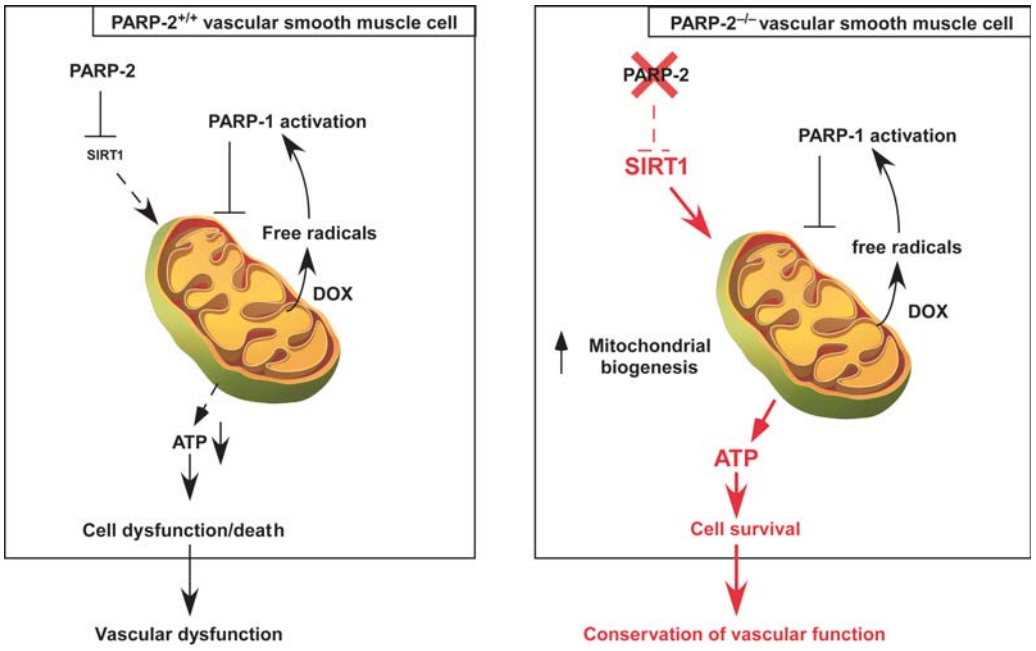

Figure 5 Proposed mechanism for PARP-2-dependent protection against DOX-evoked vascular dysfunction. DOX treatment evokes vascular dysfunction, which is mediated by an increase in free radical formation, resulting in DNA breaks, PARP-1 activation, and cellular energetic catastrophe. However, DOX-induced toxicity is partially antagonized by PARP-2 depletion. PARP-2 down-regulation evokes an increase in SIRT1 expression, which results in the activation of mitochondrial biogenesis. Elevated mitochondrial function protects aortic smooth muscle from DOX-induced toxicity without affecting PARP-1-mediated functions.

DOX-evoked endothelial dysfunction is both PARP-1- and PARP-2-independent. Cellular NAD^+ depletion was also similar in control and PARP-2-depleted cells (*Figure 2G*), suggesting again a minor, if any, role for PARP-2 in this process. Taken together, PARP-2 depletion or deletion results in vascular protection without affecting DOX-induced overall PARP activity.

3.3 SIRT1 overexpression counteracts DOX toxicity

Apparently, the protection provided by the depletion of PARP-2 has a different mechanism than the one responsible for the protective effect of PARP-1 inhibition. Mitochondrial function and structure is deteriorated upon DOX treatment.[26] Moreover, preservation of mitochondrial function is associated with protection against DOX toxicity.[27–29] These observations prompted us to investigate pathways that modulate mitochondrial function. SIRT1 is an NAD^+-dependent class III deacetylase that promotes mitochondrial biogenesis,[30–32] while PARP-2 has been identified as a repressor of SIRT1 expression.[19] Danz *et al.* have shown that pharmacological activation of SIRT1 by resveratrol enhances mitochondrial biogenesis in cardiomyocytes. Thus, induction of SIRT1 by PARP-2 depletion might be capable of counteracting the free radical-evoked mitochondrial dysfunction that occurs upon DOX treatment.[33] Accordingly, we tested whether increased SIRT1 expression might be the key protective mechanism against DOX treatment in *PARP-2*$^{-/-}$ mice.

Disruption or depletion of PARP-2 in aortas or in MOVAS cells (*Figure 3A* and *B*) resulted in an increase in *SIRT1* mRNA and SIRT1 protein levels (*Figure 3C* and *D*). This increase in SIRT1 expression was associated with the induction of the SIRT1 promoter (*Figure 3E*), which was mediated by a decrease in the occupancy of the SIRT1 promoter by PARP-2 (*Figure 3F*).

SIRT1 activation enhances mitochondrial oxidative capacity of multiple metabolic tissues.[31] We detected increased mitochondrial DNA content both in the aorta and in MOVAS cells upon the deletion or depletion of PARP-2 (*Figure 4A* and *C*). Increased mitochondrial biogenesis was further supported by increased expression of genes involved in biological oxidation (*Foxo1*, *ATP5g1*, *ndufa2*, and *ndufb5*) in aortas (*Figure 4B*). Higher expression of oxidative genes was maintained in *PARP-2*$^{-/-}$ mice even after DOX treatment compared with $^{+/+}$ mice (*Figure 4B*). To provide further evidence for the involvement of increased mitochondrial activity, mitochondrial membrane potential and oxygen consumption were determined in MOVAS cells upon DOX treatment (*Figure 4D* and *E*). Without DOX treatment, scPARP-2 and shPARP-2 MOVAS cells displayed similar mitochondrial membrane potential, but PARP-2 silencing resulted in a slightly higher oxygen consumption rate. Oxygen consumption and free radical production increased at 7 h after DOX treatment (*Figures 2B* and *4D*), suggesting mitochondrial uncoupling and mitochondrial dysfunction. Mitochondrial membrane potential in scPARP-2 MOVAS cells increased in line with the increment of DOX concentration, suggesting mitochondrial hyperpolarization (*Figure 4E*). Hyperpolarization of mitochondrial membrane has been described as an early event in apoptosis supporting impaired mitochondrial biogenesis.[34] Overall oxygen consumption was higher in shPARP-2 MOVAS cells than in scPARP-2 cells. The difference in oxygen consumption increased upon DOX treatment similarly, while mitochondrial hyperpolarization was much lower suggesting milder mitochondrial damage (*Figure 4D* and *E*).

4. Discussion

DOX toxicity affects both cardiac and vascular functions.[1] In the vasculature, DOX treatment has been shown to affect endothelial function[9] but no definitive data are available for its effect on the vascular smooth muscle and the extracellular matrix.[4,5,10] We have affirmed the deterioration of endothelial function in DOX-treated animals but it seems to be independent of both PARP-2 and PARP-1, at least 2 days post-treatment. Importantly, however, early upon DOX administration, vascular smooth muscle is also damaged. We have shown that the deletion of PARP-2 provided protection against the vascular failure induced by DOX. Moreover, this protective phenotype was linked to the preservation of vascular smooth muscle. PARP-2 depletion did not modulate the DNA breakage–PARP-1 activation–cell death pathway. Therefore, it is likely that PARP-2 does not affect PARP-1 activation that may exert its deleterious effects.

As a possible alternative protective mechanism, we have investigated the preservation of mitochondrial functions, as it has been shown to protect against DOX toxicity.[26–29,33] PARP-2 depletion has been recently associated with the induction of mitochondrial oxidation through the induction of SIRT1 expression.[19] The link between PARP-2 depletion–SIRT1 activation–enhancement of mitochondrial biogenesis was further supported by the fact that SIRT1 activation has been shown to induce mitochondrial biogenesis in various tissues.[30–32] Indeed, we have detected increased SIRT1 content after PARP-2 ablation both *in vivo* and in cultured aortic smooth muscle cells which was the consequence of the induction of the SIRT1 promoter.

The augmented expression and activity of SIRT1 caused enhanced mitochondrial biogenesis, which may have contributed to the resistance of *PARP-2*$^{-/-}$ animals against vascular DOX toxicity. It appears that higher level of mitochondrial activity provides an advantage for PARP-2-depleted cells over control cells upon oxidative stress-induced mitochondrial dysfunction (e.g. DOX treatment). Mitochondrial biogenesis, induced by PARP-2 depletion, may counterbalance the DOX-induced loss of mitochondrial activity (*Figure 5*).

To the best of our knowledge, this is the first study reporting the protective properties of SIRT1-induced mitochondrial biogenesis in blood vessels. Indeed, SIRT1 has been shown to act as a cardioprotective factor.[33,35–38] Pharmacological activation of SIRT1 by resveratrol has been demonstrated to induce mitochondrial activity in cardiomyocytes.[33] However, it must be noted that results obtained with resveratrol cannot simply be attributed to SIRT1 activation, as the specificity of resveratrol towards SIRT1 is debated.[39] Moreover, it may act as a free radical scavenger;[40] hence, it may eliminate reactive species released by DOX. Therefore, resveratrol may interfere with PARP-1 activation by quenching free radicals and hence protect mitochondria, or may act on unknown pharmacological targets to confer protection. As Danz *et al.*[33] have detected a complete loss of free radical production upon resveratrol treatment, it cannot be ruled out that resveratrol treatment acted upstream of mitochondrial biogenesis induction interfering with PARP-1 activation and provided protection through blunting PARP-1-mediated cell death.

In the heart, SIRT1 can activate other protective mechanisms. SIRT1 may deacetylate p53 and induce the expression of Bax family proteins.[41] SIRT1 may also impair PARP-1 activation and the consequent cellular dysfunction through deacetylating PARP-1[38] or by consuming NAD^+.[37] However, we did not observe differences in PARP activity or NAD^+ consumption in PARP-2-depleted smooth muscle cells or in the *PARP-2*$^{-/-}$ aorta, but observed an up-regulation of SIRT1 and increased mitochondrial protein expression and function. These apparent differences suggest that the mechanism of vascular protection may consist of different pathways than the ones observed in the heart. Importantly, however, preservation of mitochondrial function seems to be a key issue in the protection against DOX toxicity.

It is tempting to speculate that SIRT1-mediated induction of mitochondrial biogenesis may also have contributed to the protective phenotype of PARP-2 ablation in oxidative stress-mediated diseases such as colitis[16] or cerebral ischaemia[15,17] and could be exploited in other oxidative stress-related diseases. This hypothesis calls for the continuation of the development of PARP-2-specific inhibitors that may be used in such settings.[17]

In summary, here, we provide evidence for the protective role of SIRT1 in the vasculature and implicate PARP-2 as a new target to limit DOX-induced vascular damage. Furthermore, we propose that modulation of the PARP-2–SIRT1 axis to enhance mitochondrial activity may be a new therapeutic pathway to revert mitochondrial hypofunction in the cardiovascular system or in other organs.

Supplementary material

Supplementary material is available at *Cardiovascular Research* online.

Acknowledgements

We acknowledge the help of Mrs Erzsébet Herbály and Mrs Anita Jeney and the helpful corrections of György Haskó.

Conflict of interest: none declared.

Funding

This work was supported by a Bolyai fellowship to P.B. and A.T.; National Innovation Office (FR-26/2009, Baross program ÉletMent and Seahorse grants); Hungarian National Science Foundation (CNK80709, IN80481, K60780, K84300, K73003, K82009, PD83473); University of Debrecen, Medical and Health Science Center (Mecenatura Mec-8/2011); Hungarian Ministry of Health (ETT 430/2006); TÁMOP 4.2.1./B-09/1/KONV-2010-0007, TÁMOP-4.2.2/B-10/1-2010-0024 and TÁMOP-4.2.2-08/1-2008-0019 projects implemented through the New Hungary Development Plan, co-financed by the European Social Fund.

References

1. Singal PK, Iliskovic N. Doxorubicin-induced cardiomyopathy. *N Engl J Med* 1998;**339**:900–905.
2. Pacher P, Liaudet L, Bai P, Mabley JG, Kaminski PM, Virag L *et al.* Potent metalloporphyrin peroxynitrite decomposition catalyst protects against the development of doxorubicin-induced cardiac dysfunction. *Circulation* 2003;**107**:896–904.
3. Doroshow JH, Davies KJ. Redox cycling of anthracyclines by cardiac mitochondria. II. Formation of superoxide anion, hydrogen peroxide, and hydroxyl radical. *J Biol Chem* 1986;**261**:3068–3074.
4. Bai P, Mabley JG, Liaudet L, Virag L, Szabo C, Pacher P. Matrix metalloproteinase activation is an early event in doxorubicin-induced cardiotoxicity. *Oncol Rep* 2004;**11**:505–508.
5. Dawer SP, Featherstone T, Ratcliffe MA, Weir J, Dawson AA, Bennett B *et al.* Accelerated increase in aortic diameter in patients treated for lymphoma. *Heart Vessels* 1988;**4**:237–240.
6. Pedrycz A, Wieczorski M, Czerny K. The influence of a single dose of adriamycin on the pregnant rat female liver-histological and histochemical evaluation. *Ann Univ Mariae Curie Sklodowska Med* 2004;**59**:319–323.
7. Bristow MR, Minobe WA, Billingham ME, Marmor JB, Johnson GA, Ishimoto BM *et al.* Anthracycline-associated cardiac and renal damage in rabbits. Evidence for mediation by vasoactive substances. *Lab Invest* 1981;**45**:157–168.

8. Ochodnicky P, Henning RH, Buikema H, Kluppel AC, van Wattum M, de Zeeuw D *et al*. Renal endothelial function and blood flow predict the individual susceptibility to adriamycin-induced renal damage. *Nephrol Dial Transplant* 2009;**24**:413–420.
9. Murata T, Yamawaki H, Yoshimoto R, Hori M, Sato K, Ozaki H *et al*. Chronic effect of doxorubicin on vascular endothelium assessed by organ culture study. *Life Sci* 2001; **69**:2685–2695.
10. Taga I, Yamamoto K, Kawai H, Kawabata H, Masada K, Tsuyuguchi Y. The effects of intra-arterially injected adriamycin on microvascular anastomosis. *J Reconstr Microsurg* 1987;**3**:153–158.
11. Berger NA. Poly(ADP-ribose) in the cellular response to DNA damage. *Radiat Res* 1985;**101**:4–15.
12. Pacher P, Liaudet L, Bai P, Virag L, Mabley JG, Hasko G *et al*. Activation of poly(ADP-ribose) polymerase contributes to development of doxorubicin-induced heart failure. *J Pharmacol Exp Ther* 2002;**300**:862–867.
13. Pacher P, Liaudet L, Mabley JG, Cziraki A, Hasko G, Szabo C. Beneficial effects of a novel ultrapotent poly(ADP-ribose) polymerase inhibitor in murine models of heart failure. *Int J Mol Med* 2006;**17**:369–375.
14. Ame JC, Rolli V, Schreiber V, Niedergang C, Apiou F, Decker P *et al*. PARP-2, A novel mammalian DNA damage-dependent poly(ADP-ribose) polymerase. *J Biol Chem* 1999;**274**:17860–17868.
15. Kofler J, Otsuka T, Zhang Z, Noppens R, Grafe MR, Koh DW *et al*. Differential effect of PARP-2 deletion on brain injury after focal and global cerebral ischemia. *J Cereb Blood Flow Metab* 2006;**26**:135–141.
16. Popoff I, Jijon H, Monia B, Tavernini M, Ma M, McKay R *et al*. Antisense oligonucleotides to poly(ADP-ribose) polymerase-2 ameliorate colitis in interleukin-10-deficient mice. *J Pharmacol Exp Ther* 2002;**303**:1145–1154.
17. Moroni F, Formentini L, Gerace E, Camaioni E, Pellegrini-Giampietro DE, Chiarugi A *et al*. Selective PARP-2 inhibitors increase apoptosis in hippocampal slices but protect cortical cells in models of post-ischaemic brain damage. *Br J Pharmacol* 2009;**157**:854–862.
18. Menissier-de Murcia J, Ricoul M, Tartier L, Niedergang C, Huber A, Dantzer F *et al*. Functional interaction between PARP-1 and PARP-2 in chromosome stability and embryonic development in mouse. *EMBO J* 2003;**22**:2255–2263.
19. Bai P, Canto C, Brunyanszki A, Huber A, Szanto M, Cen Y *et al*. PARP-2 regulates SIRT1 expression and whole-body energy expenditure. *Cell Metab* 2011;**13**:450–460.
20. Bai P, Hegedus C, Erdelyi K, Szabo E, Bakondi E, Gergely S *et al*. Protein tyrosine nitration and poly(ADP-ribose) polymerase activation in *N*-methyl-*N*-nitro-*N*-nitrosoguanidine-treated thymocytes: implication for cytotoxicity. *Toxicol Lett* 2007;**170**:203–213.
21. Nemoto S, Fergusson MM, Finkel T. Nutrient availability regulates SIRT1 through a forkhead-dependent pathway. *Science* 2004;**306**:2105–2108.
22. Scaduto RC Jr, Grotyohann LW. Measurement of mitochondrial membrane potential using fluorescent rhodamine derivatives. *Biophys J* 1999;**76**:469–477.
23. Erdelyi K, Bai P, Kovacs I, Szabo E, Mocsar G, Kakuk A *et al*. Dual role of poly(ADP-ribose) glycohydrolase in the regulation of cell death in oxidatively stressed A549 cells. *FASEB J* 2009;**23**:3553–3563.
24. Brunyanszki A, Hegedus C, Szanto M, Erdelyi K, Kovacs K, Schreiber V *et al*. Genetic ablation of PARP-1 protects against oxazolone-induced contact hypersensitivity by modulating oxidative stress. *J Invest Dermatol* 2010;**130**:2629–2637.
25. Bai P, Houten SM, Huber A, Schreiber V, Watanabe M, Kiss B *et al*. Poly(ADP-ribose) polymerase-2 controls adipocyte differentiation and adipose tissue function through the regulation of the activity of the retinoid X receptor/peroxisome proliferator-activated receptor-gamma heterodimer. *J Biol Chem* 2007;**282**:37738–37746.
26. Yen HC, Oberley TD, Vichitbandha S, Ho YS, St Clair DK. The protective role of manganese superoxide dismutase against adriamycin-induced acute cardiac toxicity in transgenic mice. *J Clin Invest* 1996;**98**:1253–1260.
27. Hasinoff BB, Schnabl KL, Marusak RA, Patel D, Huebner E. Dexrazoxane (ICRF-187) protects cardiac myocytes against doxorubicin by preventing damage to mitochondria. *Cardiovasc Toxicol* 2003;**3**:89–99.
28. Tao R, Karliner JS, Simonis U, Zheng J, Zhang J, Honbo N *et al*. Pyrroloquinoline quinone preserves mitochondrial function and prevents oxidative injury in adult rat cardiac myocytes. *Biochem Biophys Res Commun* 2007;**363**:257–262.
29. Xu M, Ashraf M. Melatonin protection against lethal myocyte injury induced by doxorubicin as reflected by effects on mitochondrial membrane potential. *J Mol Cell Cardiol* 2002;**34**:75–79.
30. Baur JA, Pearson KJ, Price NL, Jamieson HA, Lerin C, Kalra A *et al*. Resveratrol improves health and survival of mice on a high-calorie diet. *Nature* 2006;**444**: 337–342.
31. Lagouge M, Argmann C, Gerhart-Hines Z, Meziane H, Lerin C, Daussin F *et al*. Resveratrol improves mitochondrial function and protects against metabolic disease by activating SIRT1 and PGC-1alpha. *Cell* 2006;**127**:1109–1122.
32. Rodgers JT, Lerin C, Haas W, Gygi SP, Spiegelman BM, Puigserver P. Nutrient control of glucose homeostasis through a complex of PGC-1alpha and SIRT1. *Nature* 2005; **434**:113–118.
33. Danz ED, Skramsted J, Henry N, Bennett JA, Keller RS. Resveratrol prevents doxorubicin cardiotoxicity through mitochondrial stabilization and the Sirt1 pathway. *Free Radic Biol Med* 2009;**46**:1589–1597.
34. Scarlett JL, Sheard PW, Hughes G, Ledgerwood EC, Ku HH, Murphy MP. Changes in mitochondrial membrane potential during staurosporine-induced apoptosis in Jurkat cells. *FEBS Lett* 2000;**475**:267–272.
35. Alcendor RR, Gao S, Zhai P, Zablocki D, Holle E, Yu X *et al*. Sirt1 regulates aging and resistance to oxidative stress in the heart. *Circ Res* 2007;**100**:1512–1521.
36. Borradaile NM, Pickering JG. NAD(+), sirtuins, and cardiovascular disease. *Curr Pharm Des* 2009;**15**:110–117.
37. Pillai JB, Isbatan A, Imai S, Gupta MP. Poly(ADP-ribose) polymerase-1-dependent cardiac myocyte cell death during heart failure is mediated by NAD+ depletion and reduced Sir2alpha deacetylase activity. *J Biol Chem* 2005;**280**:43121–43130.
38. Rajamohan SB, Pillai VB, Gupta M, Sundaresan NR, Konstatin B, Samant S *et al*. SIRT1 promotes cell survival under stress by deacetylation-dependent deactivation of poly (ADP-ribose) polymerase 1. *Mol Cell Biol* 2009;**26**:4116–4129.
39. Pacholec M, Bleasdale JE, Chrunyk B, Cunningham D, Flynn D, Garofalo RS *et al*. SRT1720, SRT2183, SRT1460, and resveratrol are not direct activators of SIRT1. *J Biol Chem* 2010;**285**:8340–8351.
40. Lorenz P, Roychowdhury S, Engelmann M, Wolf G, Horn TF. Oxyresveratrol and resveratrol are potent antioxidants and free radical scavengers: effect on nitrosative and oxidative stress derived from microglial cells. *Nitric Oxide* 2003;**9**:64–76.
41. Zhang C, Feng Y, Qu S, Wei X, Zhu H, Luo Q *et al*. Resveratrol attenuates doxorubicin-induced cardiomyocyte apoptosis in mice through SIRT1-mediated deacetylation of p53. *Cardiovasc Res* 2011;**90**:538–545.